Planning Hull Hydrodynamics

Study of the Effects Caused by Variation of the Thrust Line Due to Displacement

Series 62 Model No. 4667-1

Researcher/ Author:	Matthew Ricciardo, BSE, University of Michigan, Naval Architecture and Marine Engineering
Editor:	Christopher Fuller, BSE, University of Michigan, Mechanical Engineering, Naval Architecture and Marine Engineering

Subject:	Series 62 Model 4667-1 Thrust Line Analysis
Date:	March 1, 2010
Revision:	0

Abstract

This paper addresses the influence of the thrust line on the ships hydrostatic and hydrodynamic characteristics, and the relevance of this topic to waterjet prediction methods. Savitsky developed a method for predicting resistance, based on prismatic planing hull data, to address the effect of propeller thrust on the heave and pitching moment of the hull. Savitsky's method incorporates seakeeping measurement techniques and energy moment equations to establish equilibrium points. However waterjets had not been considered as part of these experiments.

Previous papers that focus on the waterjet system do not provide much insight to the optimization of the hull-waterjet system. The placement of the waterjet nozzle is determined by the waterline of the ship. The nozzle placement directly affects the efficiency of a planing hull due to the moment created by the thrust and total resistance. Thus, a waterjet propulsion system is a function of the ship's displacement, center of gravity, and hull form.

Once the ship reaches a planing speed, the hydrostatic forces become less substantial as the hydrodynamic forces increase. Displacement hulls, such as destroyers and patrol vessels, are sensitive to changes in displacement, trim, and thrust line. Those parameters directly affect the stability, resistance, effective power, running trim, and heave.

This study is an extension of the planing hull data that has been studied for the past 50 years. In this experiment, the hull form and the vertical center of gravity are isolated. The Series 62 model is used to test the effects of waterjets by adjusting the displacement, trim, and thrust line.

M.A. Ricciardo
matthew.ricciardo@gmail.com

Table of Contents

List of Figures

List of Tables

M.A. Ricciardo
matthew.ricciardo@gmail.com

List of Abbreviations and Definitions

a_C	Maximum amplitude	L_{OA}	Length overall
a	Distance from CG to D_f (measured normal to D_f)	L_P	Projected chine length
A_S	Area of whisker spray in the plane perpendicular to keel	l_P	Distance to the center of pressure
A_{WS}	Whisker spray area	L_{WS}	Length of whisker spray
b	Wetted beam length	N	Normal (Savitsky)
B_{PA}	Breadth over chines	P_E	Effective power
B_{PX}	Maximum breadth over chines	R_{AIR}	Air resistance
c	Distance from CG to N (measured normal to N) ($c = LCG - l_P$)	R_e	Reynolds number
C_{AA}	Air resistance coefficient	R_S	Whisker spray resistance
C_{AIR}	Air roughness coefficient	R_T	Total resistance (measured)
C_f	Schoenherr turbulent friction coefficient	R_W	Wave resistance
C_F	Friction drag coefficient	S	Total pressure area
C_{Form}	Form drag coefficient	S_S	Area of pressure area in the plane perpendicular to keel
$C_{L\beta}$	Deadrise surface lift coefficient	T	Thrust
C_{lo}	Zero deadrise surface lift coefficient	t	Thrust deduction factor
C_P	Coefficient of the center of pressure	TL	Thrust Line (runs parallel with the baseline and positive up above keel)
C_T	Total resistance coefficient	V	Forward speed
C_S	Whisker spray resistance coefficient	V_1	Average bottom velocity
C_R	Residuary resistance coefficient	VCG	Vertical center of gravity above the keel
C_V	Speed coefficient (Volumetric Froude #)	x	Distance from CG to R_T (measured normal to R_T)
C_W	Wave resistance coefficient		
d	Depth at transom	α	Angle between keel and stagnation line in the horizontal plane (degrees)
D_f	Total drag resistance (Savitsky)	β	Deadrise angle (degrees)
D_F	Friction drag	Δ	Displacement
D_{Form}	Form drag	λ	Mean wetted length to beam ratio
f	Distance from CG to thrust line (measured normal to TL)	π	Phi
F_n	Froude number	ρ	Density of fresh water
g	Gravity	τ	Running trim angle
h_i	Elemental prism height (measured in lab)	μ	Dynamic viscosity of water
L	Wetted length	θ	Angle between the forward edge of the whisker spray and the keel (degrees)
L_c	Chine wetted length	Θ	Angle between the forward edge of the whisker spray and the keel (degrees)
LCG	Longitudinal center of gravity measured from the bow at baseline	η_3	Heave
L_k	Keel wetted length	ν	Kinematic viscosity

M.A. Ricciardo
matthew.ricciardo@gmail.com

Introduction

The International Tow Tank Committee developed guidelines to ensure consistency of practices and processes for laboratory model tests. ITTC – Recommended Procedures and Guidelines, document number 7.5-02-05-01, details the methodology of the testing methods and data acquisition for resistance tests of a planing mono-hull. Model testing is done to determine the total resistance, find porpoising limit, and refine the final design.

Empirical equations can aid preliminary design and are the fundamentals of high speed craft conception. Empirical equations for the total resistance are categorized into five components: friction drag, form drag, wave resistance, whisker spray resistance and air resistance.

The composition of these five components are listed below:

1. Friction drag is a composition of the ITTC 1957 friction line, mean wetted length, beam width, speed, deadrise, running trim, surface roughness, and Reynolds number.
2. Form drag is a composition of hull form, weight, speed, deadrise, running trim, and viscosity. Form drag is found experimentally.
3. Wave resistance is a composition of wetted surface, beam width, speed, deadrise, running trim, and Froude number.
4. Whisker spray resistance is a composition of speed, running trim, beam width, and bow form.
5. Air resistance is a composition of air draft, beam width, and speed.

These components are independently calculated but are conjoined by individual characteristics of the hull. There is a commonality among the five components: beam width, speed, and running trim. Any change to these characteristics will have a direct effect on all components of the total resistance.

The thrust line has a direct correlation with the five components of the total resistance. The thrust line is a function of the thrust moment and total resistance moment. The thrust line is primarily affected by speed and running trim, thus altering the wetted area. The thrust moment is also a function of the thrust line. The thrust line for a waterjet system is dependent on the transom depth because of pump priming.

Most of the total resistance is composed of friction drag and wave resistance. It is the primary responsibility of the designer to decrease these two components of resistance. Keep in mind as friction and wave resistance decrease; form drag, whisker spray and air resistance will become more predominant at planing speeds.

Model Testing

1.1 Testing Facilities

Testing was conducted in the University of Michigan Marine Hydro Laboratory (MHL). The MHL tow tank – which is approximately 360 ft in length, 22 ft wide and over 10 ft deep – is equipped with a carriage that can reach speeds of 20 ft/s. The carriage is equipped with a 64 bit, multichannel, data acquisition system and planing dynamometer. The dynamometer's servo-motor maintained the thrust line parallel with the keel during the test. The model was restricted by the dynamometer and yoke; therefore yaw, sway, surge, and roll are all zero.

The data acquisition system recorded elemental prism height, running trim, trim, and total resistance using a linear variable differential transducer, inclinometer, accelerometer, and load cell respectively. The carriage is equipped with a speedometer to measure speed. In order to minimize error, the placidity of the water was measured using a laser displacement sensor ahead of the model. The equipment was calibrated using the highest scientific standards to minimize error.

1.2 Model Characteristics: Series 62 Model 4667-1

The Series 62 is a pure-planing hull, with a wide transom and convex bow, is ideal for waterjet applications. The series 62 is not as susceptible to the loss of buoyancy caused by waterjets, allowing for greater loading of the forward portion. The Series 62 Model 4667-1 was initially developed and tested by Eugene Clement and Donald Blount, and documented in a 1963 report entitled *Resistance Tests of a Systematic Series of Planing Hull Forms*.

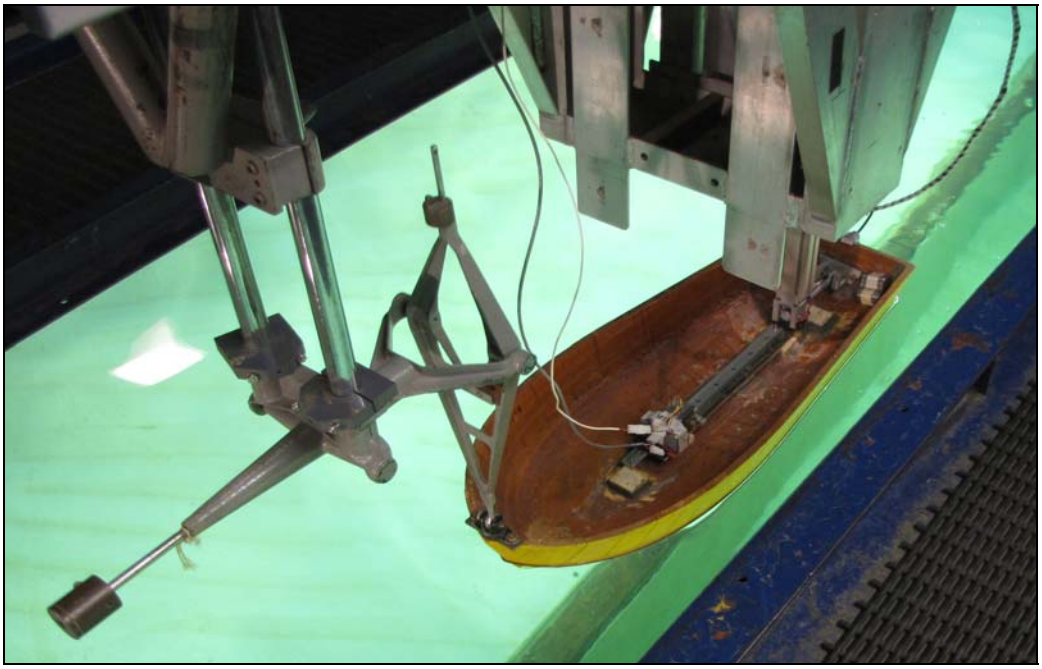

Figure 1. Series 62 Model No 4667-1 attached to MHL dynamometer

M.A. Ricciardo
matthew.ricciardo@gmail.com

Clement's and Blount's research did provide insight and guidance during the laboratory testing. The data analysis closely follows ITTC and Savitsky's method. The model used in the laboratory is shown in Figure 1 and detailed in the table below.

Series 62 Model 4667-1			
Length Overall	L_{OA}	3.721	ft
Projected planing area	A_P	3.322	ft
Mean breadth over chines	B_{PA}	0.949	ft
Breadth over chines transom	B_{PT}	0.810	ft
Deadrise	β	12.5	deg
	L_P/B_{PX}	3.06	
	B_{PX}/B_{PA}	1.21	
Projected chine length	L_P	3.50	ft
Max. breadth over chines	B_{PX}	1.144	ft
	L_P/B_{PA}	3.69	
	L_P/B_{PT}	4.32	
	B_{PT}/B_{PX}	0.71	
Centroid of A_P, % L_P fwd. of transom		48.2	% L_P
LCG aft of centroid of A_P		5.0	% L_P
Displacement 1		18.87	Lbs
Displacement 1 Thrust Line		1.566	Inches above BL
Displacement 2		22	Lbs
Displacement 2 Thrust Line		0.732 & 1.566	Inches above BL
Displacement 3		25	Lbs
Displacement 3 Thrust Line		0.766 & 1.566	Inches above BL
Each displacement was run at 0, 1, and 2 degrees trim at the bow.			

Table 1. Model Characteristics

2 Savitsky Method

Savitsky's method was first introduced to estimate the powering requirements for small planing craft in the 1960's. This data extrapolation method has been used to expand on the knowledge base of planing craft to include planing-surface lift, whisker spray drag, wetted area, pressure distributions, impact forces, wake shape, spray formation, dynamic stability, and stern flaps.

The free body diagram seen in Figure 2 has a running trim angle (τ) and measured chine wetted length (L_c) and keel wetted length (L_k). The total drag force (D_f), normal (N), and propeller thrust (T) are calculated for the planing hull in equilibrium. The resistance, thrust, and normal force are used to balance the moments with respect to the longitudinal center of gravity (LCG) and wetted area (Almeter 93). Since each quantity affects the trim, calculations for thrust must be iterated for the set trim angle to determine a balancing of the moments.

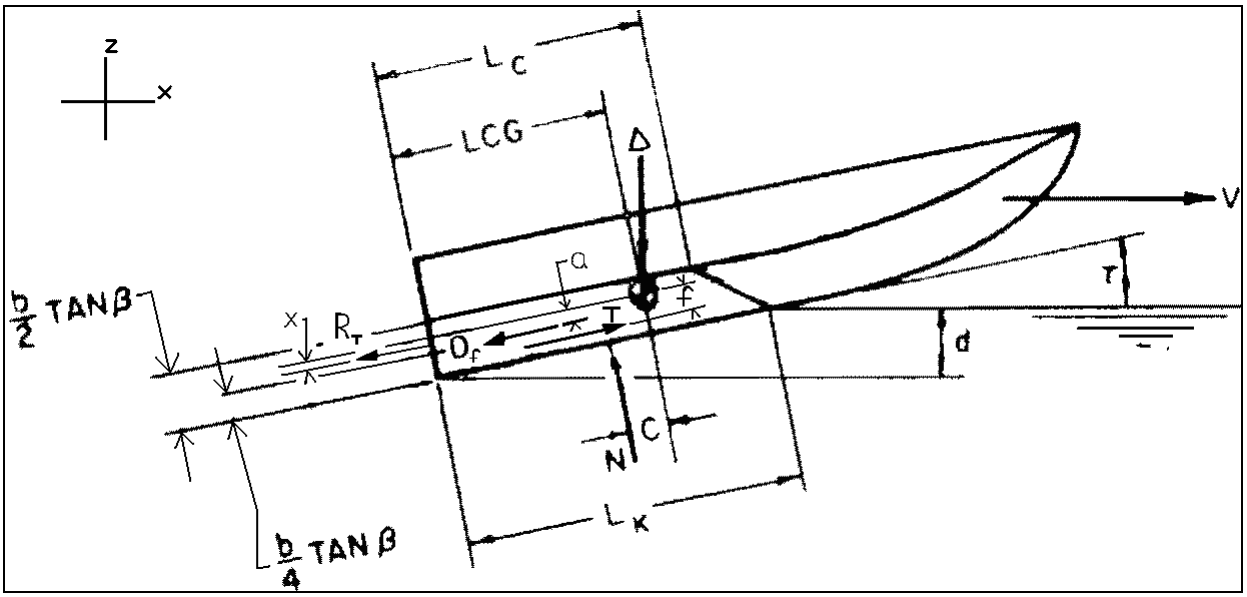

Figure 2. Force diagram of Savitsky planing hull (Savitsky 1964)

In Figure 2, D_f and N compose the total resistance (R_T). The total resistance is further detailed in Section 3.2.

Summing the horizontal and vertical forces of the force diagram respectively,

$$\sum F_X = T \cdot \cos\tau - N \cdot \sin\tau - D_f \cdot \cos\tau = 0 \qquad \textbf{Equation 1}$$

$$\sum F_X = T \cdot \cos\tau - R_T \cdot \cos\tau = 0 \qquad \textbf{Equation 2}$$

and

$$\sum F_Z = T \cdot \sin\tau + N \cdot \cos\tau - D_f \cdot \sin\tau - \Delta = 0 \qquad \textbf{Equation 3}$$

$$\sum F_Z = T \cdot \sin\tau + R_T \cdot \sin\tau - \Delta = 0 \qquad \textbf{Equation 4}$$

Summing the moments about the center of gravity:

$$\sum M = N \cdot c + D_f \cdot a - T \cdot f = 0 \qquad \textbf{Equation 5}$$

$$\sum M = R_T \cdot x - T \cdot f = 0 \qquad \textbf{Equation 6}$$

This equation holds true as long as the thrust line and total drag resistance are below the *VCG* and *N* is aft of the *LCG*. The theoretical values herein are based on Savitsky's prismatic hull as outlined in his paper *Hydrodynamic Design of Planing Hulls* (Savitsky 1964).

3 Data Analysis

3.1 Drag and Resistance Analysis

The total resistance of a ship is composed of five primary components: *friction drag*, *form drag*, *wave resistance, whisker spray resistance,* and *air resistance*.

3.1.1 Friction Drag

The acceleration of the fluid creates a viscous shear stress on the surface of the hull, producing a force known as friction drag (D_F). Friction drag is dependent on the Reynolds number and independent of the hull form because of the direct relationship with viscosity. Friction drag is approximated as a flat plate of equal length and wetted area. The empirical formula is commonly used is:

$$D_F = \frac{\rho \cdot C_f \cdot V_1^2 \cdot \left(\lambda \cdot b^2\right)}{\left(2 \cdot \cos\beta\right)^4} \qquad \textbf{(Savitsky 1964)} \qquad \textbf{Equation 7}$$

Where the mean wetted length to beam ratio (λ) is detailed in Section 3.3, C_f is the Schoenherr turbulent friction coefficient and V_1 is the average bottom velocity.

$$C_f = \frac{0.075}{\left(\log_{10} R_e - 2\right)} \qquad \textbf{(ITTC 2002)} \qquad \textbf{Equation 8}$$

$$V_1 = V \cdot \sqrt{1 - \frac{0.012 \cdot \tau_{radians}^{1.1}}{\sqrt{\lambda} \cdot \cos\tau}} \qquad \textbf{(Savitsky 1964)} \qquad \textbf{Equation 9}$$

At low trim angles, friction drag is predominant while at high trim angles, form drag is predominant (Savitsky 1964).

3.1.2 Form Drag

The acceleration of fluid creates a pressure force on the surface of the hull, producing a force known as form drag (D_{Form}). Form drag is dependent on Froude number because of the direct relationship with trim angle and hull form. The difference in resistance between the curves (R_T/Δ) represent the drag component due to viscous drag (Savitsky 1964) for trim between zero and one degree and one and two degrees trim, see Figure 3. Proceeding is an example, (R_T/Δ) for a displacement of 25 lbs and a thrust line 0.766 inches above the keel.

M.A. Ricciardo
matthew.ricciardo@gmail.com

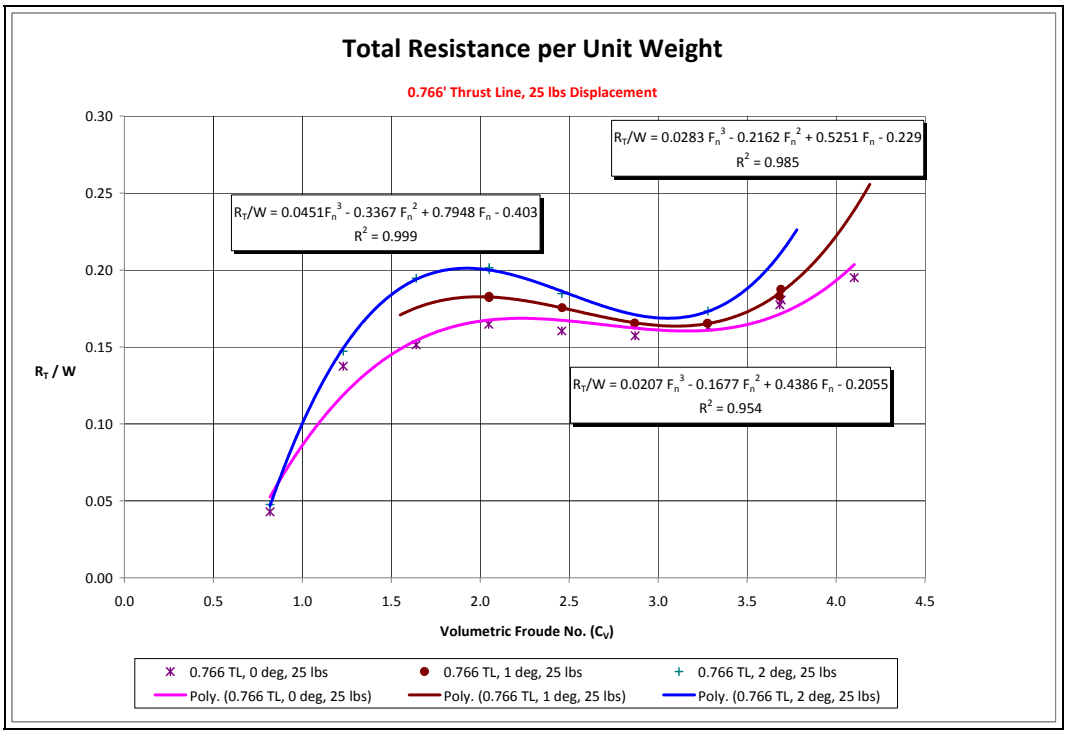

Figure 3. Total Resistance per Unit Weight vs. Froude Number

For tests conducted at 25 lbs displacement with a thrust line moment arm of 0.766 inches above the keel.
At $\tau = 2$ degrees the total resistance per unit weight: $R_T/W = 0.0451 C_V^3 - 0.3367\ C_V^2 + 0.7948\ C_V - 0.403$
At $\tau = 1$ degrees the total resistance per unit weight: $R_T/W = 0.0283\ C_V^3 - 0.2162\ C_V^2 + 0.5251\ C_V - 0.229$
At $\tau = 0$ degrees the total resistance per unit weight: $R_T/W = 0.0207\ C_V^3 - 0.1677\ C_V^2 + 0.4386\ C_V - 0.206$

The following table calculates the form drag per unit weight. As seen in Figure 3, the form drag is minimal below one ($C_V < 1$) and is negligible below 0.75 ($C_V < 0.75$).

Form Drag Calculations (for 25 lbs displacement and 0.766 inch thrust line above keel)

	Trim		25 Lbs Displacement		Total	Form Drag	
	$0<\tau<1$	$1<\tau<2$	$0<\tau<1$	$1<\tau<2$	Resistance	$0<\tau<1$	$1<\tau<2$
C_V	R_T/W	R_T/W	R_T (Lbs)	R_T (Lbs)	R_T (Lbs)	Percent of total drag	
1.5	0.0228	0.0161	0.5694	0.4031	3.6234	15.71%	11.13%
2	0.0163	0.0178	0.4075	0.4450	4.1625	9.79%	10.69%
2.5	0.0084	0.0096	0.2094	0.2406	4.1578	5.04%	5.79%
3	0.0047	0.0042	0.1175	0.1050	3.9975	2.94%	2.63%
3.5	0.0110	0.0141	0.2744	0.3531	4.0697	6.74%	8.68%

Table 2. Form Drag Calculations

At lower speeds form drag only accounts for 10-16 percent of the total drag. At higher speeds form drag can account for as much as 5-10 percent of the total drag. Turbulence will cause deviations from the ideal flow at high speed ($C_V > 3.5$).

3.1.3 Wave Resistance

The transfer of energy from the motion of the hull to the generation of waves is called wave resistance (R_W). Wave resistance is dependent on Froude number dominated by gravitational forces. The restoring forces designed into the hull form are weight and buoyancy distribution.

For low Froude numbers, the wave resistance coefficient is proportional to F_n^4:

$$C_W = \frac{R_W}{\frac{1}{2} \cdot \rho \cdot V^2 \cdot S} \cong F_n{}^4 \qquad \textbf{(Savitsky 1964)} \qquad \textbf{Equation 10}$$

Constructive and destructive interference from waves at different Froude numbers will cause the resistance coefficient to oscillate about the F_n^4. The wave resistance is simplified to:

$$R_W = \frac{1}{2} \cdot \rho \cdot V^2 \cdot S \cdot C_W \cong \Delta \tan \tau \qquad \textbf{(Savitsky 1964)} \qquad \textbf{Equation 11}$$

Where ρ is the water density and S is the total pressure area seen in Figure 4:

$$S = \frac{S_S}{\cos \beta} = \frac{b}{\cos \beta \cdot \cos \tau} \cdot \left(L_K - \frac{1}{2} L_2 \right) \qquad \textbf{(Savitsky 1964)} \qquad \textbf{Equation 12}$$

And L_K and L_2 are detailed in Section 3.3.

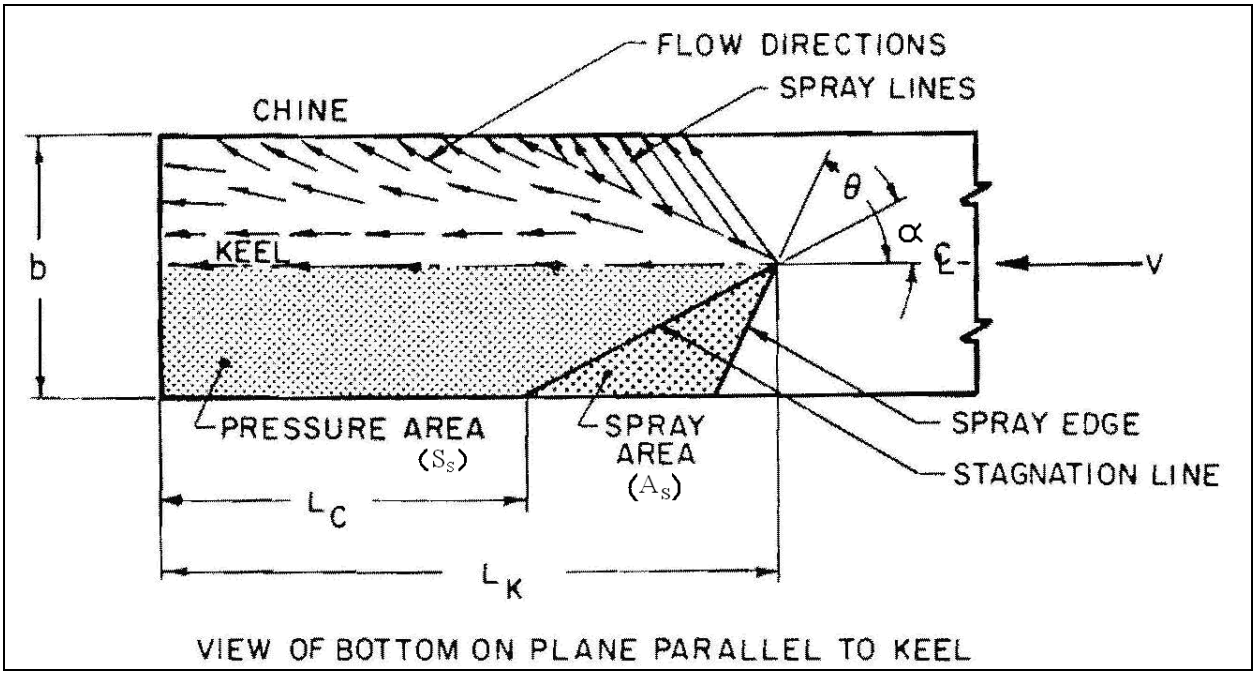

Figure 4. Flow direction along prismatic hull and surface areas (Savitsky 1964)

M.A. Ricciardo
matthew.ricciardo@gmail.com

3.1.4 Whisker Spray Resistance

Droplets that form forward of the stagnation line that runs between L_k and L_c are known as whisker spray. Whisker spray resistance is dependent on the Reynolds number because of the direct relationship with viscosity. Viscous forces caused by the whisker spray resistance (R_S) has negligible effect on lift force but adds drag resistance (Savitsky 2006).

The wetted area in the plane of the bottom surface of the hull is:

$$A_{WS} = \frac{A_S}{\cos\beta} = \frac{b^2}{4 \cdot \sin 2\alpha \cdot \cos\beta} \qquad \textbf{(Savitsky 2006)} \qquad \textbf{Equation 13}$$

Where A_S is the area of whisker spray in the plane perpendicular to keel, see Figure 4. As α approaches zero, the spray projection is perpendicular to the drag component; thus no added drag due to the spray develops.

The total viscous force caused by the whisker spray in the plane of the water level is:

$$R_S = \frac{1}{2} \cdot \rho \cdot V^2 \cdot A_{WS} \cdot C_{f_{WS}} \cdot \cos\Theta \cdot \cos\tau \qquad \textbf{(Savitsky 2006)} \qquad \textbf{Equation 14}$$

where $\cos\Theta \cdot \cos\tau$ is the vector angle component in the plane of the level water surface and θ is the angle between the foward edge of the whisker spray and the keel $\left(\Theta = \frac{\theta}{\cos\beta}\right)$ (Savisky 2006). $C_{f_{WS}}$ is the Schoenherr friction coefficient for the whisker spray which differs from coefficient used for the wetted area in Section 3.1.1. Whisker spray is a triangular free stream with a spray length (L_{WS}):

$$L_{WS} = \frac{b}{4 \cdot \sin 2\alpha \cdot \cos\beta} \qquad \textbf{(Savitsky 2006)} \qquad \textbf{Equation 15}$$

and Reynolds number for the whisker spray is:

$$R_{e_{WS}} = \frac{V \cdot L_{WS}}{\nu} \qquad \textbf{(Savitsky 2006)} \qquad \textbf{Equation 16}$$

Since the Reynolds number is small when the whisker spray is in a laminar and transitional phase, whisker spray is categorized by the Reynolds critical number ($R_{eWSCRIT}$).

$$1.5 \times 10^5 < R_{e_{WSCRIT}} < 1.5 \times 10^6$$

M.A. Ricciardo
matthew.ricciardo@gmail.com

$$C_{f_{WS}} = \frac{0.074}{\sqrt[5]{R_e}} - \frac{R_{e_{WSCRIT}}}{R_e} \qquad \textbf{(Savitsky 2006)} \qquad \textbf{Equation 17}$$

which simplifies to:

$$C_{f_{WS}} = \frac{1.328}{\sqrt{R_{e_{WS}}}} \qquad \textbf{(Savitsky 2006)} \qquad \textbf{Equation 18}$$

For $R_{e_{WS}} < 1.5 \times 10^6$ for laminar flow and

$$C_{f_{WS}} = \frac{0.074}{\sqrt[5]{R_{e_{WS}}}} - \frac{4800}{R_{e_{WS}}} \qquad \textbf{(Savitsky 2006)} \qquad \textbf{Equation 19}$$

For $R_{e_{WS}} \geq 1.5 \times 10^6$ for transitional flow.

3.1.5 Air Resistance

Although an important aspect, the prismatic model equations do not account for air drag (Troesch 1992). Without wind influence, the velocity of the air is the forward speed of the hull. The air resistance (R_{AIR}) is:

$$R_{AIR} = \frac{1}{2} \cdot \rho_{AIR} \cdot V_{AIR}^2 \cdot A_{AWL} \cdot C_{AIR} \qquad \textbf{(ITTC 2002)} \qquad \textbf{Equation 20}$$

Where C_{AIR} is the roughness coefficient an A_{AWL} is the area above the waterline. The air resistance coefficient is:

$$C_{AA} = \frac{R_{AIR}}{\frac{1}{2} \cdot \rho_{AIR} \cdot V_{AIR}^2 \cdot A_{AWL}} \qquad \textbf{(ITTC 2002)} \qquad \textbf{Equation 21}$$

Only at low Froude numbers ($C_V < 0.5$) can air resistance be neglected. Aerodynamic designs can reduce drag significantly depending on the size of the superstructure and operating speed.

M.A. Ricciardo
matthew.ricciardo@gmail.com

3.2 Total Resistance

Defining components of the total resistance is helpful in determining the effect each one will have when the thrust line and displacement are altered. The total resistance (R_T) is the summation of the friction drag, form drag, wave resistance, whisker spray resistance, and air resistance.

$$R_T = D_F + D_{Form} + R_W + R_S + R_{AIR} \quad \textbf{Equation 22}$$

Expanding the equation:

$$R_T = \frac{\rho \cdot V_1^2 \cdot C_f \cdot \lambda \cdot b^2}{2 \cdot \cos\beta \cdot \cos\tau} + D_{Form} + \Delta \tan\tau + \frac{1}{2} \cdot \rho \cdot V^2 \cdot C_{f_{WS}} \cdot \frac{b^2 \cos\Theta \cdot \cos\tau}{4 \cdot \sin 2\alpha \cdot \cos\beta} + R_{AIR} \quad \textbf{Equation 23}$$

By replaceing $\Delta\lambda = \frac{\cos\Theta}{4 \cdot \sin 2\alpha \cdot \cos\beta}$ with Figure 5, the whisker spray resistance is simplified.

The simplified equation for the total resistance is:

$$R_T = \frac{\rho \cdot V_1^2 \cdot C_f \cdot \lambda \cdot b^2}{2 \cdot \cos\beta \cdot \cos\tau} + D_{Form} + \Delta \tan\tau + \frac{1}{2} \cdot \rho \cdot V^2 \cdot C_{f_{WS}} \cdot b^2 \cdot \Delta\lambda \cdot \cos\tau + R_{AIR} \quad \textbf{Equation 24}$$

The figure shows a point where $\Delta\lambda$ equals zero. At this point the whisker spray is perpendicular to the keel and the drag contribution will be equal to zero.

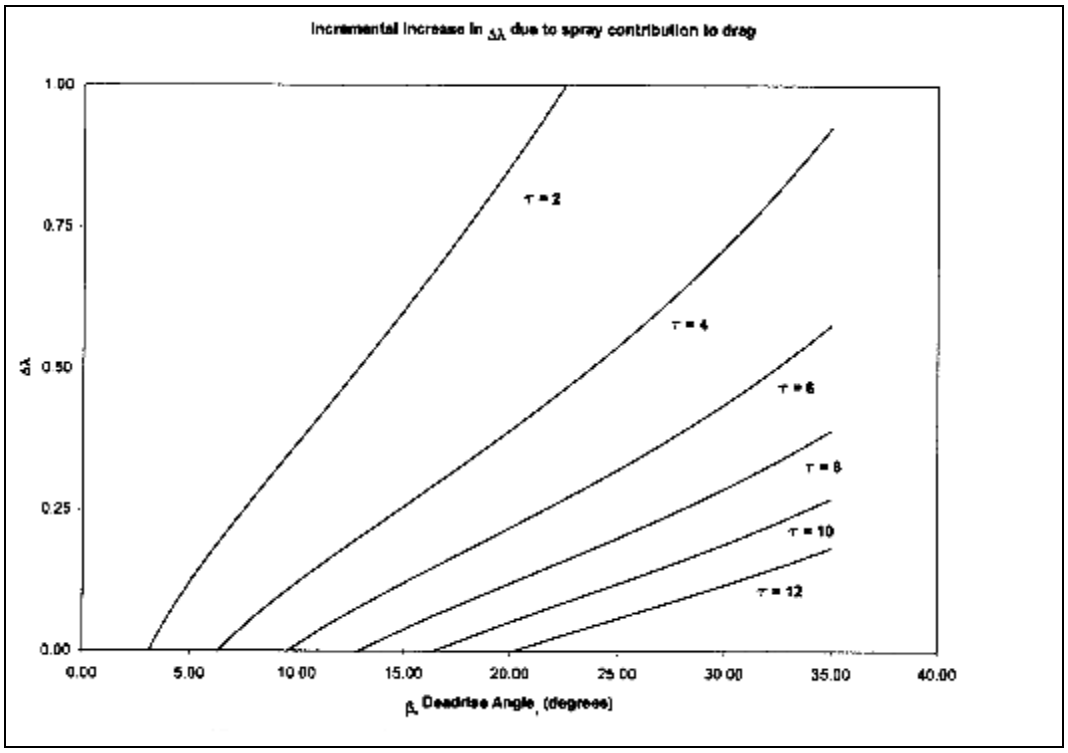

Figure 5. Incremental increase in $\Delta\lambda$ for spray contribution due to running trim (Savitsky 2006)

The total resistance coefficient (C_T) is:

$$C_T = C_F + C_{Form} + C_W + C_S + C_{AA} \qquad \textbf{Equation 25}$$

Air Drag, form drag, and wave resistances are dependent on Froude number while friction drag and whisker spray resistance are dependent on the Reynolds number:

$$C_T = C_F(R_e) + C_{Form}(F_r) + C_W(F_r) + C_S(R_e) + C_{AA}(F_r) \qquad \textbf{Equation 26}$$

To simplify, the residuary resistance coefficient (C_R) is the combined form drag and wave resistance.

$$C_T = C_F(R_e) + C_S(R_e) + C_R(F_r) + C_{AA}(F_r) \qquad \textbf{Equation 27}$$

Previous studies have shown the total resistance of a ship is dependent on the ship length (L), beam (B), and speed (V) in calm water. The total resistance is then a function of f_1 as follows:

$$R_T = f_1(\rho, V, L, g, \mu) \qquad \textbf{Equation 28}$$

M.A. Ricciardo
matthew.ricciardo@gmail.com

The total resistance coefficient is nondimensionalized as follows:

$$C_T = f_1\left(\frac{\rho \cdot V \cdot L}{\mu}, \frac{V}{\sqrt{g \cdot L}}\right) \qquad \textbf{Equation 29}$$

The function (f_1) is composed of the

Reynolds number $\left(R_e = \frac{\rho \cdot V \cdot L}{\mu}\right)$ **(Equation 30)** and *Froude number* $\left(F_r = \frac{V}{\sqrt{g \cdot L}}\right)$ **(Equation 31).**

The total resistance coefficient is:

$$C_T = \frac{R_T}{\frac{1}{2} \cdot \rho \cdot V^2 \cdot S} \qquad \textbf{(ITTC 2002)} \qquad \textbf{Equation 32}$$

The total resistance is a result of *inertial forces* (acceleration of the fluid), *body forces* (due to gravity) and *viscous forces* (effects of fluid viscosity); where the Reynolds number is the ratio of the inertial forces to the viscous forces, and the Froude number is the ratio of the inertial forces to gravity forces. Thus, the total resistance coefficient is a hulls unique combination of dimensionless ratio of resistance forces to inertial forces.

3.3 Wetted Length Analysis

The Volumetric Froude number also known as the speed coefficient (C_V):

$$C_V = \frac{V}{\sqrt{g \cdot \left(\frac{\Delta}{\rho}\right)^{1/3}}} \qquad \textbf{(Savitsky 1964)} \qquad \textbf{Equation 33}$$

A prismatic hull is planing when $C_V > 1.2$, according to Savitsky.

The recorded wetted lengths are the distance from the stern to the intersection of the keel and mean water line (L_k), and the distance from the stern to the edge of the spray root along the chine (L_c), see Figure 6.

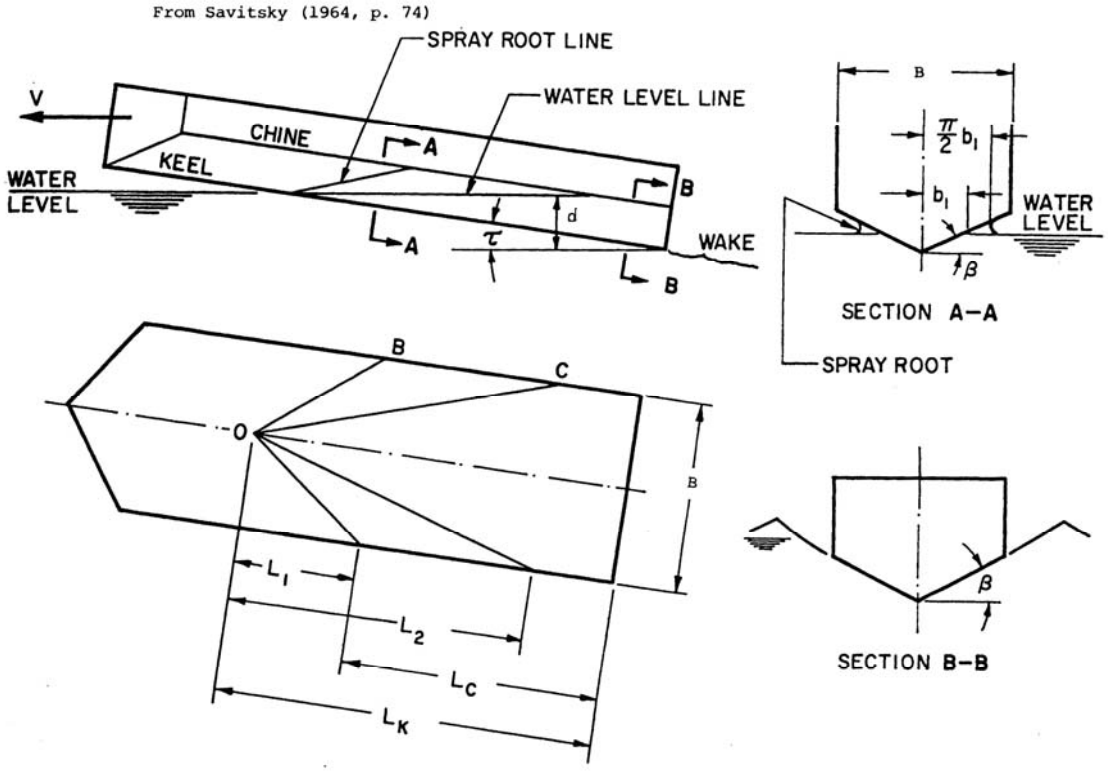

Figure 6. Definitions of a Planing Hull (Savitsky 1964)

The measured values (L_k and L_c) are used to calculate the calm water intersection (L_2) and spray root intersection (L_1) of the chine.

$$L_2 = \frac{b}{2} \cdot \frac{\tan\beta}{\tan\tau} \qquad \textbf{(Savitsky 1964)} \qquad \textbf{Equation 34}$$

M.A. Ricciardo
matthew.ricciardo@gmail.com

$$L_1 = L_k - L_c = \frac{b}{\pi} \cdot \frac{\tan\beta}{\tan\tau} \qquad \textbf{(Savitsky 1964)} \qquad \textbf{Equation 35}$$

where *b* is the wetted beam. The measured wetted keel length is approximately:

$$L_k \approx \frac{d}{\sin\tau} \qquad \textbf{(Savitsky 1964)} \qquad \textbf{Equation 36}$$

The wetted chine length is approximately:

$$L_c \approx \frac{d}{\sin\tau} - \frac{b}{\pi}\frac{\tan\beta}{\tan\tau} \qquad \textbf{(Savitsky 1964)} \qquad \textbf{Equation 37}$$

where *d* is the water depth at the transom. The empirical equations for (L_c) and (L_k) are only valid for a speed coefficient of two or greater ($C_V > 2$), deadrise less than 15 degrees ($\beta < 15^o$), and trim less than 4 degrees ($\tau < 4^o$). Savitsky's approximations are verified using measurements taken from an underwater camera.

Using the preceding values for each run, the mean wetted length-beam ratio (λ) is:

$$\lambda = \frac{L_k + L_c}{2b} \qquad \textbf{(Savitsky 1964)} \qquad \textbf{Equation 38}$$

Between speed coefficients of 3.5 and 4.0 porpoising occurs. This is observed by the spray roots curving along the hull and vibrations recorded in the data. Porpoising can be avoided by reducing the speed and moving the center of gravity of the ship forward, thus decreasing the trim (Faltinsen, 2005).

M.A. Ricciardo
matthew.ricciardo@gmail.com

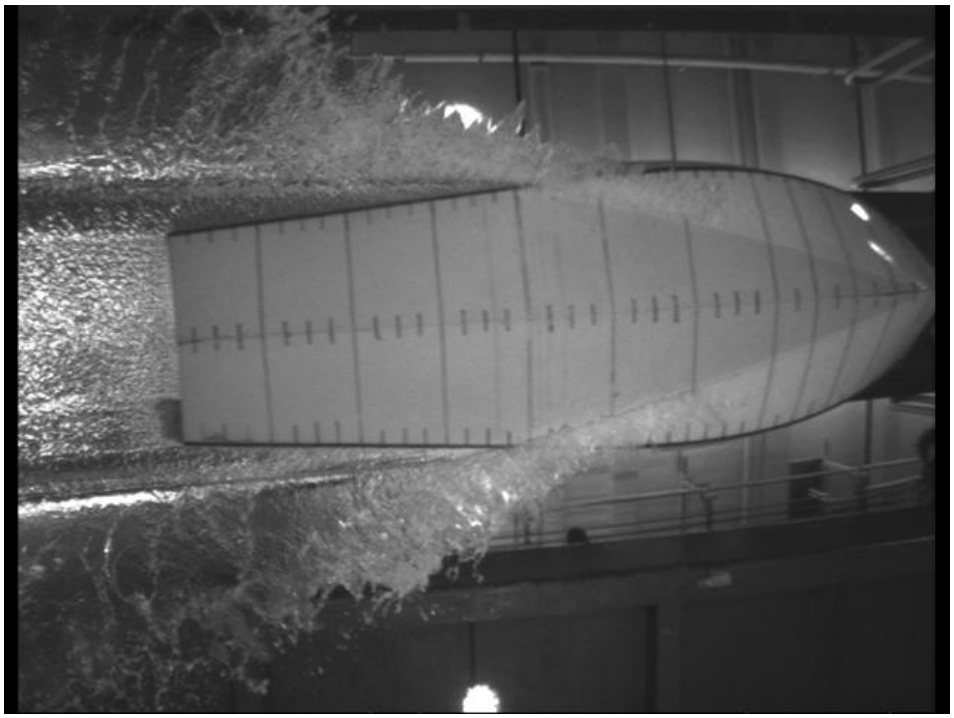

Figure 7. Pure planing (C_V = 3.789) model speed 19.5 ft/s

The pure planing regime is from approximately $3.25 < C_V$ and greater. In the pure planing regime hydrodynamic forces are dominant. A fully developed 'rooster tail' was visible behind the hull. The transom and chine are dry. The difference between L_k and L_c is at its greatest and whisker spray is negligible. The model had minimal wetted area but maximum dynamic lift, and the running trim trended to four degrees. Waves are present only behind the model caused by a void created by the transom. Porpoising begins to occur in this regime.

M.A. Ricciardo
matthew.ricciardo@gmail.com

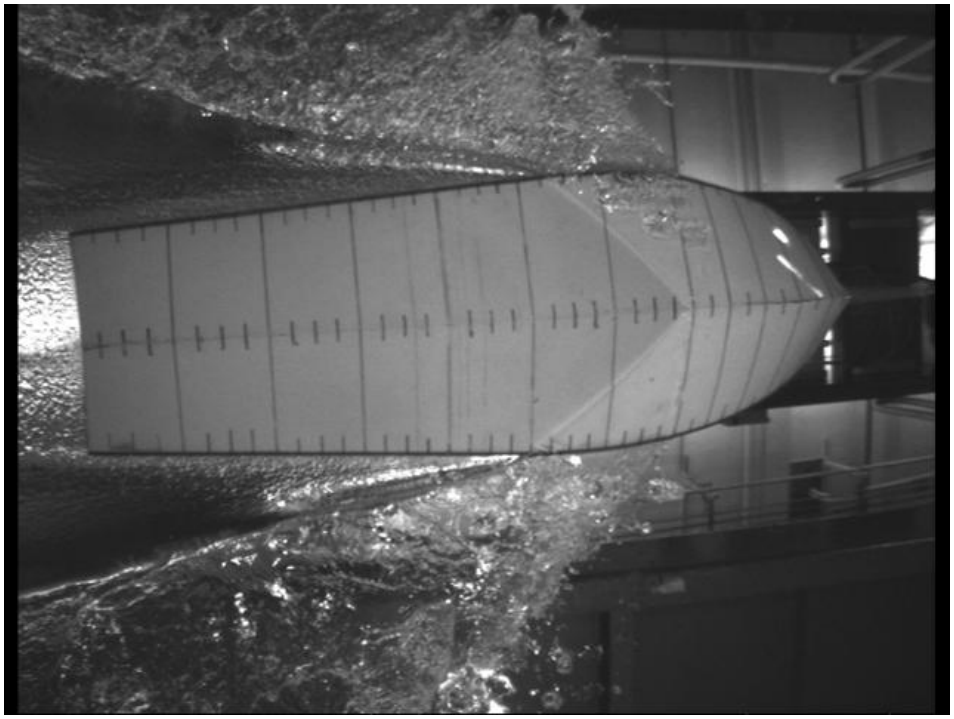

Figure 8. Planing (C_V = 2.048) model speed 10 ft/s

The planing regime is from approximately $1.75 < C_V < 3.25$. In the planing regime, hydrostatic forces become less substantial as the dynamic lift increases. The transom and chine are wetted by turbulent flow. Substantial waves are present from the keel and due to the void behind the model, and running trim angle climaxes in the planing regime. Bow waves cause significant drag and a 'rooster tail' began to develop behind the hull.

Flow separation from the chine does not occur when:

$$\lambda < \frac{\tan\beta}{2 \cdot \pi \cdot \tau_{radians}} \qquad \textbf{(Faltinson 2005)} \qquad \textbf{Equation 39}$$

And low speed flow separation from the chines will start when $\frac{b}{2}$ satisfies:

$$\frac{b}{2} = \frac{\pi}{2 \cdot \tan\beta} \cdot L_1 \cdot \tau_{radians} \Rightarrow 1 = \frac{\tau_{radians}}{\tan\tau} \qquad \textbf{(Faltinson 2005)} \qquad \textbf{Equation 40}$$

M.A. Ricciardo
matthew.ricciardo@gmail.com

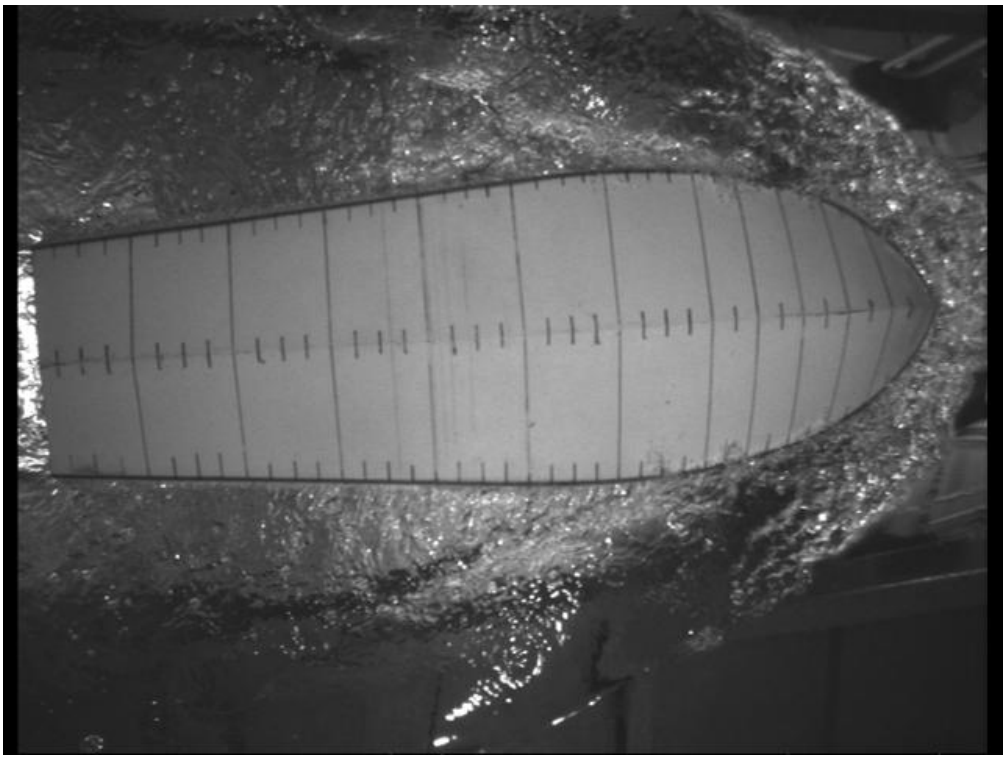

Figure 9. Pre-planning (C_V = 0.819), model speed 4 ft/s

The pre-planing regime is from approximately $0.5 < C_V < 1.75$. This is approximately up to the hump speed. In the pre-planing regime hydrostatic forces dominant. The chine and transom are wet. L_k is equal to L_c; therefore, there is no whisker spray. Water pile-up at the bow is present. This causes waves to form at the bow and along the chine. Turbulent flow is present behind the transom.

M.A. Ricciardo
matthew.ricciardo@gmail.com

3.4 Center of Pressure Analysis

Two approximations are used to estimate the center of pressure. First, the centroid of the dynamic component is assumed to be 75 percent of the mean wetted length forward of the transom. Second, the centroid of the buoyant force is assumed to be 33 percent forward of the transom (Savitsky 1964). The distance from the transom forward to the center of pressure (l_P) is:

$$l_P = C_P \cdot \lambda \cdot b \qquad \textbf{Equation 41}$$

The coefficient of the center of pressure (C_P) is;

$$C_P = 0.75 - \frac{1}{5.21 * \frac{C_V{}^2}{\lambda^2} + 2.39} \qquad \textbf{Equation 42}$$

Hydrostatic loads and the effect of free surface wave generation are implicitly included in the formula (Faltinson 2005). The center of pressure is decoupled from the initial trim and hull form, and is a function of speed and wetted length. The pressure on the bottom of the hull creates lift which is then summarized using the following lift coefficients.

The deadrise surface lift coefficient ($C_{L\beta}$) is:

$$C_{L\beta} = \frac{\Delta}{\frac{1}{2}\rho \cdot V^2 b^2} \qquad \textbf{(Savitsky 1964)} \qquad \textbf{Equation 43}$$

The zero deadrise-lift coefficient (C_{Lo}) is then calculated by solving $C_{L\beta}$

$$C_{L\beta} = C_{Lo} - 0.0065\beta \cdot C_{Lo}{}^{0.60} \qquad \textbf{(Savitsky 1964)} \qquad \textbf{Equation 44}$$

When C_{lo} is solved, the mean wetted length to beam ratio (λ) can be rewritten:

$$\lambda = \frac{L_k + L_c}{2b} = \frac{C_{lo}}{\tau_{radians}^{1.1}} \qquad \textbf{(Savitsky 1964)} \qquad \textbf{Equation 45}$$

3.5 Heave Analysis

Hydrodynamic lift is caused by the pressure build up in front of the hull. The vertical distance component is called heave. Heave (η_3) is the result of wave generation and directly linked to wave resistance. Heave is sensitive to hull form and dependent on the Froude number.

M.A. Ricciardo
matthew.ricciardo@gmail.com

The elemental prism height (h_i) is the vertical distance the transom rises from equilibrium. Heave is a combination of the elemental prism height and the center of pressure as seen in Figure 10 and by the following equation.

$$\eta_3 = h_i + L_K \cdot \sin\tau = h_i + d \qquad \textbf{Equation 46}$$

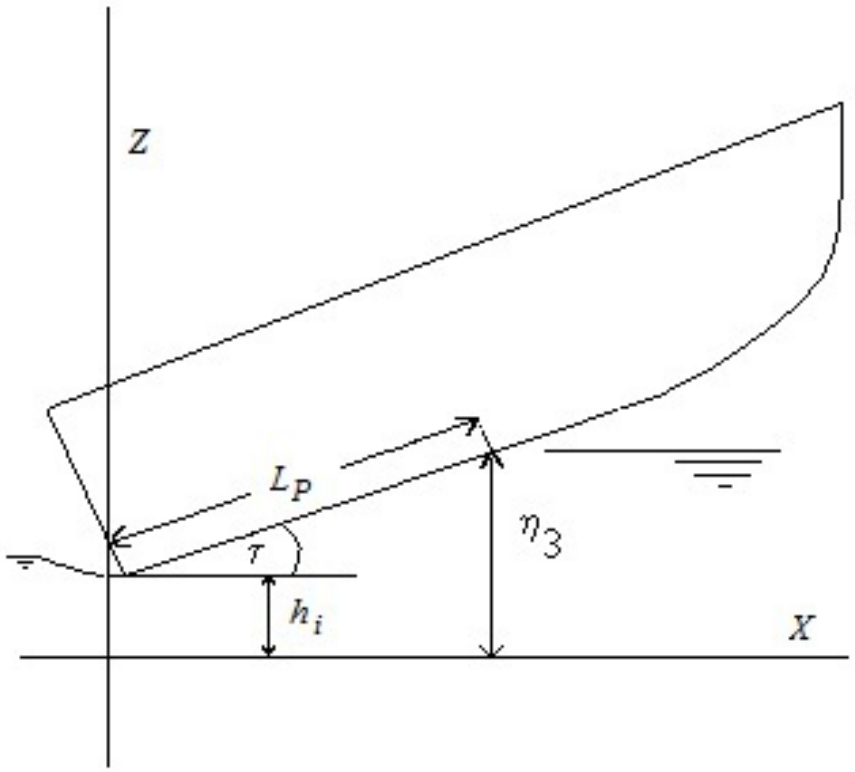

Figure 10. Diagram of Heave

The hydrodynamic lift is then characterized by the added mass coefficient as documented by Ikeda 2000, Faltinsen 2011, Ibrahim 2010 and other authors.

4 Test Data Results

4.1 Resistance

The ideal model weight is between 22 to 24 pounds with zero trim. This range is where the hump in the resistance curve is negligible in the planing regime. The hump in the resistance curve is primarily caused by wave resistance. As speed increases, the bow wave begins to diminish. The bow wave is primarily caused by trim and hull form.

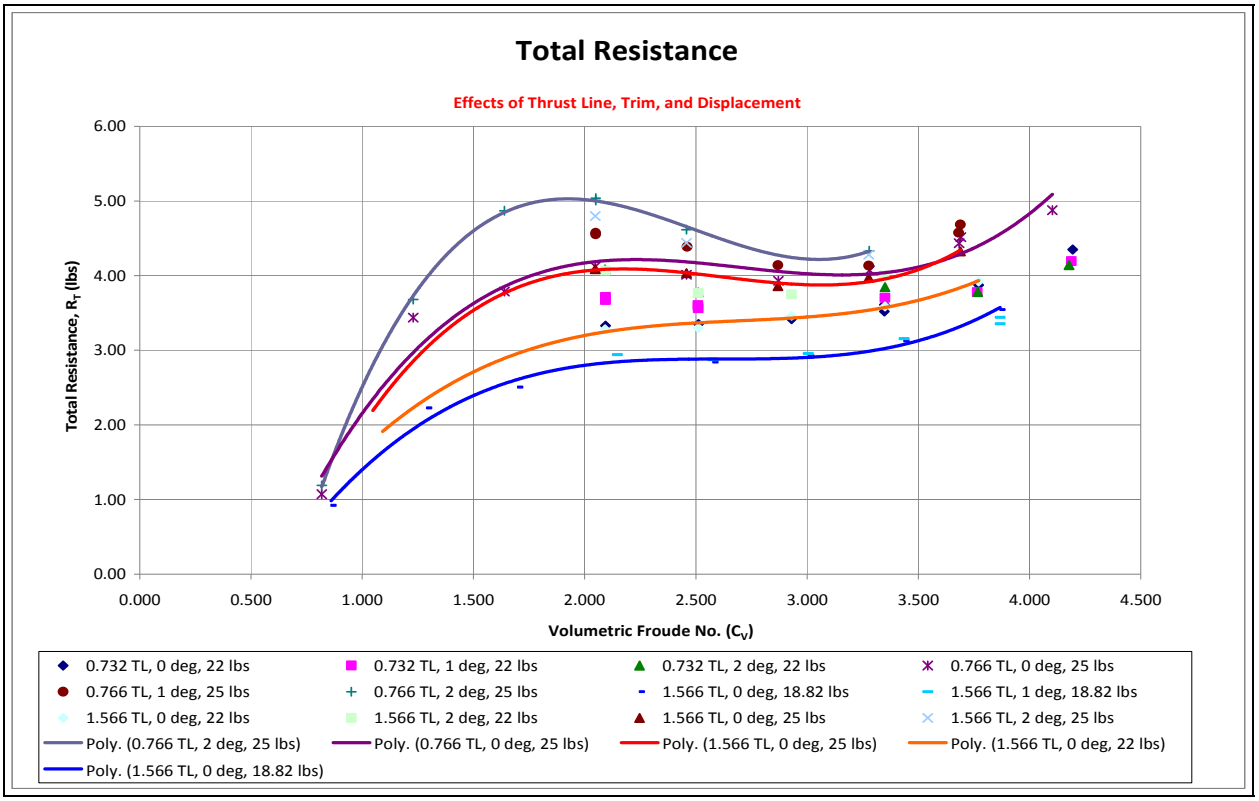

Figure 11. Total Resistance vs. Froude Number: Effects of Thrust Line, Trim, and Displacement

The thrust line accounts for less than a 3% change in the total resistance. Increasing the thrust line shifts the resistance curves right, allowing for less resistance at higher speeds in the pre-planing and planing regime. Trim and displacement are the main factors for the total resistance as seen in Figure 11. This is verified by the empirical equations in Section 3.1.

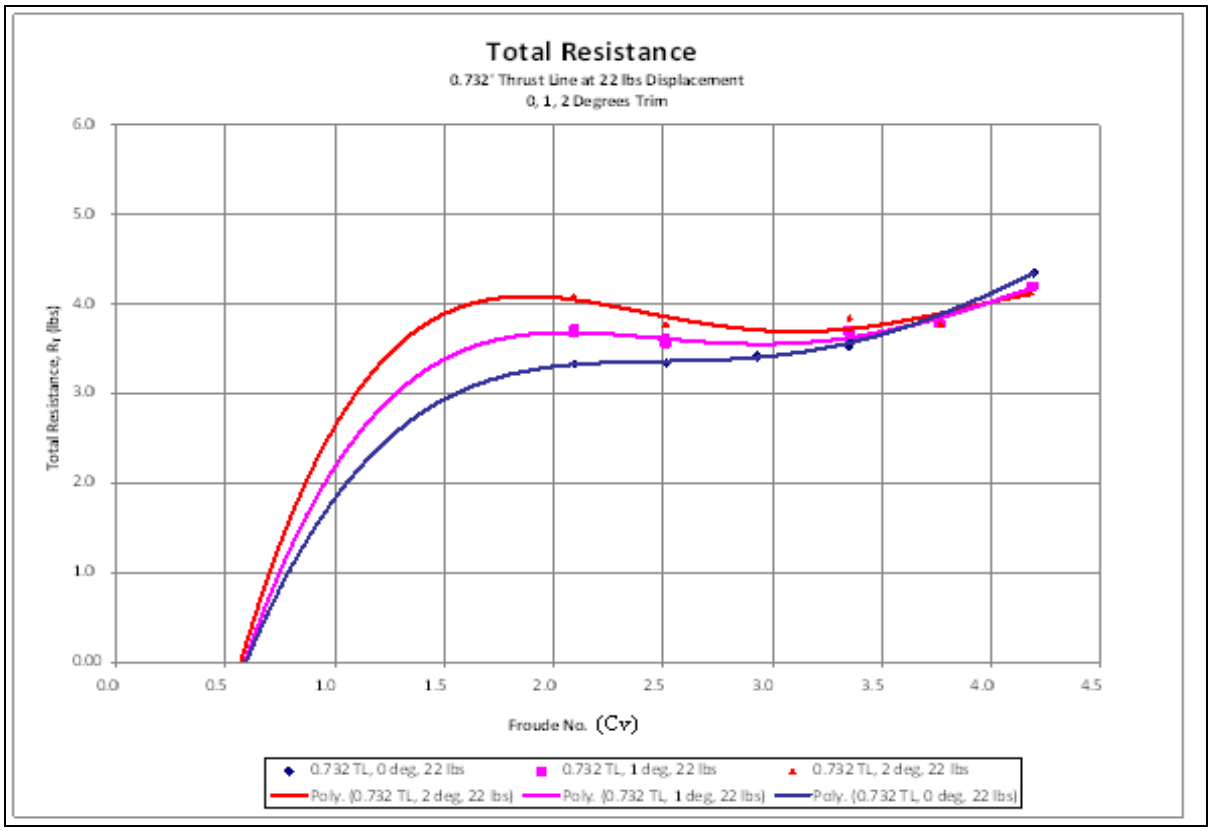

Figure 12. Total Resistance vs. Froude Number at 22 lbs Displacement

Adjusting the trim alone will cause a significant increase in resistance as seen in Figure 12. In other words, moving the *LCG* aft will increase the resistance of the hull. Flare of the stern is the best method to control the *LCG* from a hull design standpoint.

M.A. Ricciardo
matthew.ricciardo@gmail.com

4.2 Running Trim Angle

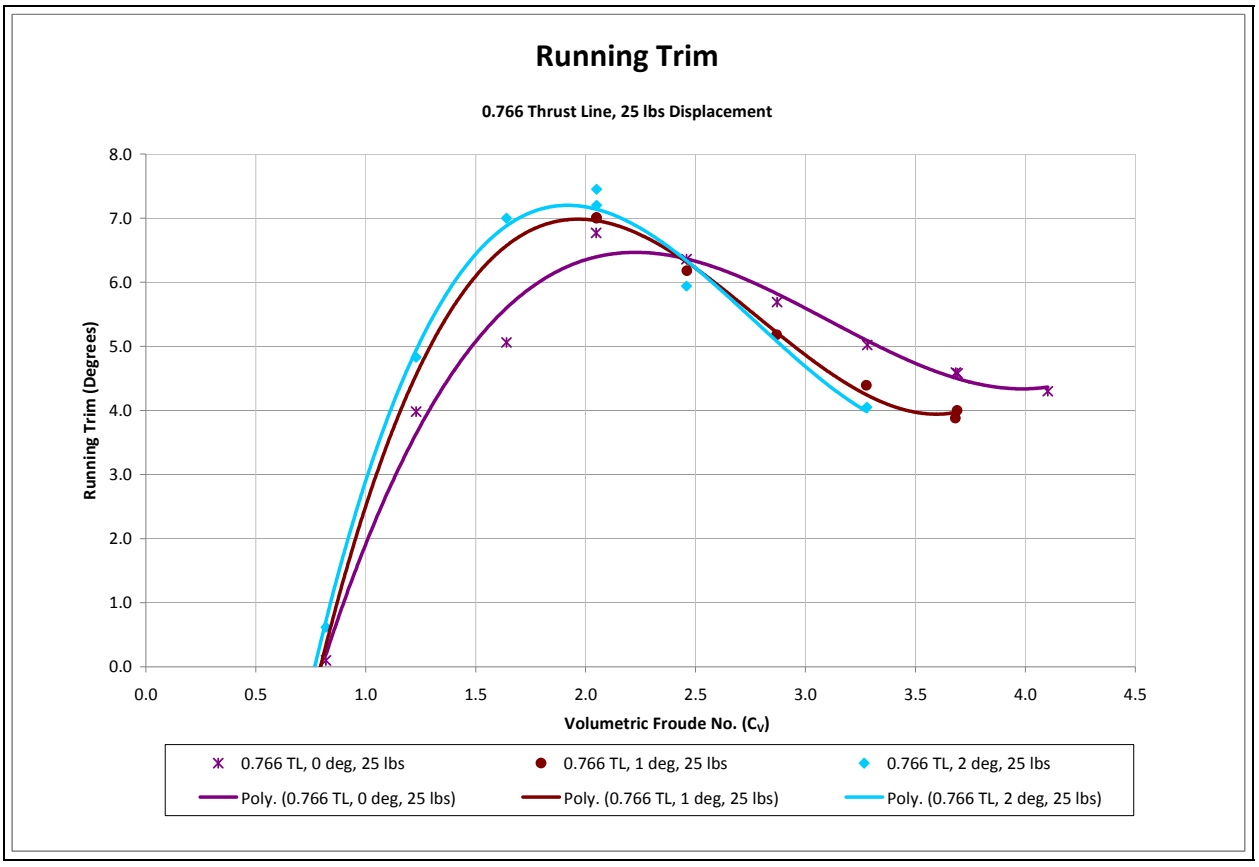

Figure 13. Running Trim vs. Froude Number at 0, 1, and 2 Degrees Trim

Increasing the trim caused the amplitude of the running trim and total resistance to increase. Trim is a less significant factor for the running trim as seen in Figure 13. Displacement and thrust line are the main factors influencing the running trim. Running trim has a significant contribution to the wave resistance.

M.A. Ricciardo
matthew.ricciardo@gmail.com

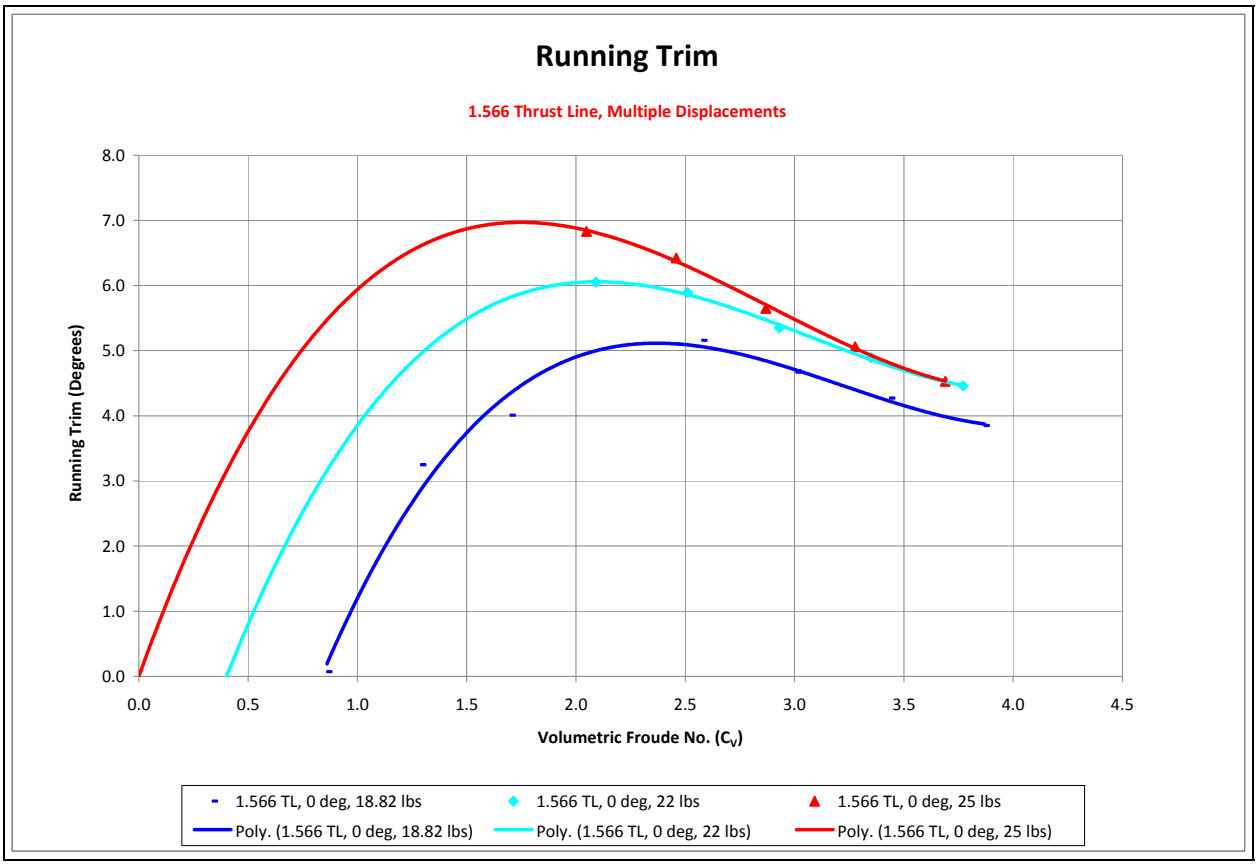

Figure 14. Running Trim vs. Froude Number at Multiple Displacements

Decreasing the displacement causes decreased amplitude and belays the running trim (see Figure 14). The wetted area and heave have a direct correlation with displacement and running trim. The coupled heave and pitch motion are root components of porpoising.

A similar response is seen when the thrust line is changed at speeds below $C_V < 2.75$. Increasing the thrust line without changing the displacement decreases the amplitude and prolongs the onset of higher running trim. The correlation between the thrust line and running trim, coupled with heave, is not implicitly explained by the empirical equations. The correlation is caused by the change in moment of the thrust component in Equation 3.

As the running trim increases, the *VCG* moves up with proportion to heave, thus increasing *f*. It is desired to minimize the running trim. This will, in return, minimize the total resistance without increasing the thrust required. From Equation 3, it is concluded:

$$f = VCG - TL \qquad \textbf{Equation 47}$$

assuming *TL* is parallel with the keel.

M.A. Ricciardo
matthew.ricciardo@gmail.com

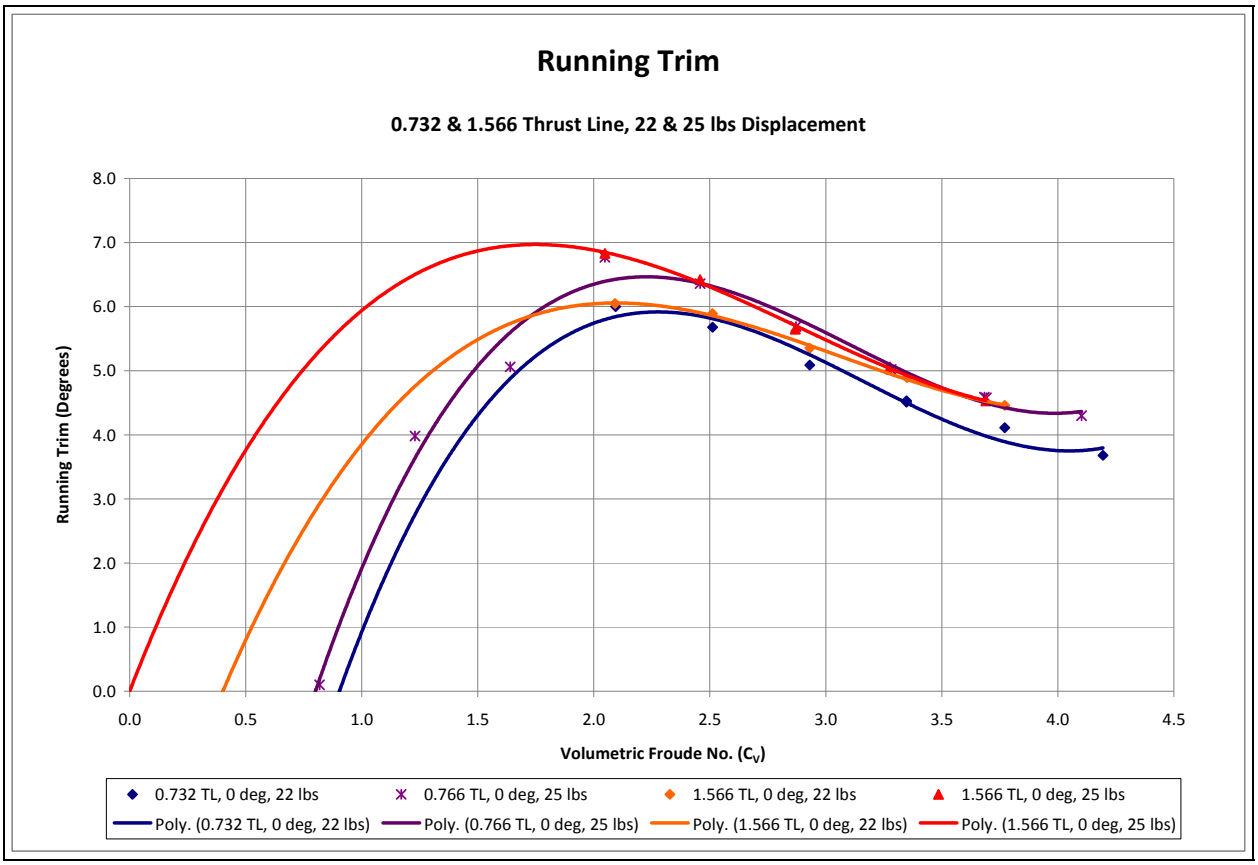

Figure 15. Running Trim vs. Froude Number: Effect of the Thrust Line and Displacement

When comparing thrust line and displacement (Figure 15), it was discovered that the thrust line has a significant effect to the running trim but not at high speeds, as anticipated. The effect occurs at speeds below the Froude number of 3.0 due to the hydrodynamic lift.

4.3 Waterjet Propulsion

A waterjet is treated as a void filled with water and the thrust line of the nozzle is dependent on the aft draft for pump priming reasons. Hydrostatics then determine the trim and longitudinal center of gravity (LCG) of the vessel. Machinery selection has a significant role in the displacement of the vessel.

The effective power (P_E) is the total power required to propel the hull, which is the product of the total resistance and forward speed.

$$P_E = V \cdot R_T = \frac{1}{2} \cdot C_T \cdot \rho \cdot V^3 \cdot S \qquad \textbf{(Faltinsen 2005)} \qquad \textbf{Equation 48}$$

This is the power required at the waterjet opening. This value does not include losses due to suction loss, impeller cavitation, or mechanical efficiency.

M.A. Ricciardo
matthew.ricciardo@gmail.com

The waterjet thrust is:

$$T = \frac{R_T}{(1-t)} \qquad \textbf{(Zubaly 1996)} \qquad \textbf{Equation 49}$$

Where (1-*t*) is the thrust deduction factor:

At high speeds, the running trim merges. This concludes that at high speed near the porpoising limit running trim is not affected by the thrust line. Since the normal force moves aft with an increase in speed, minimizing *c* will decrease porpoising.

From Equation 6 and 49, we seek the optimum thrust line (TL) that will satisfy the moments.

$$TL = VCG - \frac{R_T \cdot x}{T} \qquad \textbf{Equation 50}$$

Or it can simply be written $TL = VCG - x \cdot (1-t)$. Since priming is required, the thrust line can be labeled as a function of the transom depth so that:

$$TL = \frac{1}{2} \cdot d \qquad \textbf{Equation 51}$$

where ½ is an arbitrary number, open for the designer or manufacturer requirements. In the experiment three thrust lines were used, as seen in the preceding figures, 0.732", 0.766" and 1.566" above the baseline.

As the weight of the model increases, the normal force increases; thus, there is an increase in transom depth and the height required for the waterjet. It is desired to minimize the total resistance without increasing the thrust required. Since the normal force moves aft with an increase in speed, minimizing *c* and *a* will optimize the thrust line.

M.A. Ricciardo
matthew.ricciardo@gmail.com

5.0 Conclusion

Any instability due to irregularities of the spray roots could be analyzed as higher order motions. These oscillations were consequently ignored and is common practice due to the complexity of analysis (Troesch 1992). It was observed at high Froude numbers, high amplitude oscillations composed of coupled heave and pitch motions, also known as porpoising. During porpoising, the data recorded was unusable.

The friction drag, form drag, and wave resistance are most influenced by the thrust line, trim, and displacement. When planing, the total resistance peaked at planing speed while the wetted area decreases due to hydrodynamic lift. This caused the running trim angle to decrease, thus reducing the wave resistance on the hull. Altering the trim angle significantly affected the normal force. The normal force is the resulting pressure force acting perpendicular to the bottom. Since *f* is dependent on the aft draft (and the draft is a function of the center of gravity and displacement) of the vessel, which by design, can be optimized by proper trimming and sizing of the total wetted surface.

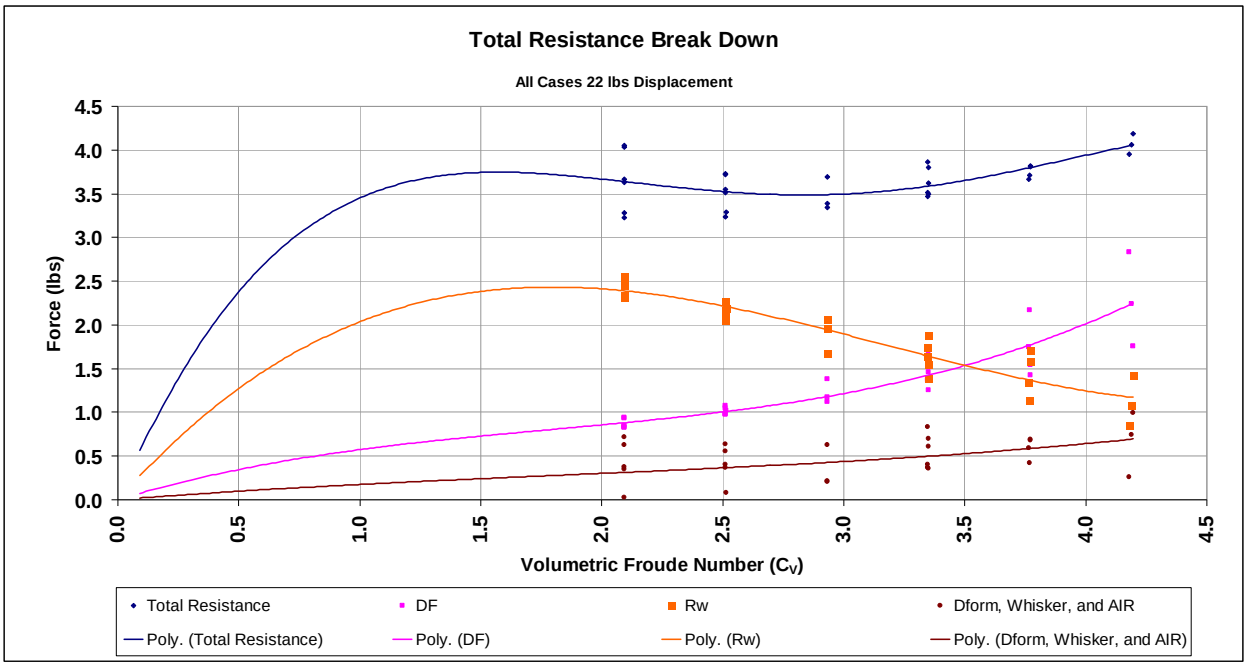

Figure 16. Total Resistance Break Down (22 lbs Displacement): Total Resistance (R_T), Friction Drag (D_F), Wave Resistance (R_W) and Residual Resistance (D_{form}, Whisker, and Air Resitance)

Figure 16 diagrams the total resistance. The total resistance is segmented into three main categories: friction drag, wave resistance, and residual resistance which consists of form drag, whisker spray resistance and air resistance. Form drag, whisker spray resistance and air resistance are grouped together due to their direct relationship with the forward speed. As speed increases; form drag decreases, air resistance increases and whisker spray resistance increases with increased speed in the pre-planing regime but decreases with increased speed in the planing regime.

Where:

- The pre-planing regime ($0.5 < C_V < 1.75$) wave resistance is the dominant drag component.
- The planing regime ($1.75 < C_V < 3.25$) wave resistance and friction drag are the dominant drag component.
- The pure planing regime ($C_V > 3.25$) friction drag is the dominant drag component.

As previously detailed in Section 3.3.

The maximum operating speed is $C_V = 3.5$ where the wave resistance is equal to the friction drag. Porpoising occurs after this speed. Positive static trim will shift this point vertically up. Changing the thrust line will also shift this point vertically. Changing the displacement will shift this operating speed horizontally.

The thrust line could have significant effects to the maneuverability of the hull. Testing was not conducted to measure these values but past research suggests there are trade-offs between waterjet propulsion and propellers. The data presented serves as a guideline for the placement of the waterjet propulsion unit.

6.0 References

Faltinsen, O. (2005). *Hydrodynamics of high-speed Marine Vehicles*. New York: Cambridge.

Clement E.P, Blount D.L; *Resistance tests of a systematic series of planing hull forms*; SNAME transcript; 1963

Shacham D, Yang S.I; *The effect of transom flaps on planing boat performance*; NA520 Advance Model Testing; Aug 1975

Troesch, A; *On the Hydrodynamics of Vertically Oscillating Planing Hulls.* Journal of Ship Research, Vol. 36, No. 4 Dec. 1992, pp. 317-331

Savitsky, D; *Hydrodynamic design of planing hulls*; Marine Technology; Oct 1964 pp 71-95

Harvald, S. A. *Resistance and Propulsion of Ships*, John Wiley and Sons, NY (1982).

Olson, R. M. and Wright, S. J. *Essentials of Engineering Fluid Mechanics*, Fifth Edition, Harper & Row, Publishers, Inc. (1990).

Principles of Naval Architecture, Edward V. Lewis, Editor, Society of Naval Architects and Marine Engineers, Jersey City, NJ, 1988.

PNA Vol. II	page 7-18, 22-34	Types of Resistance
	page 57-60	EHP Extrapolation

Savitsky, D, DeLorme, M, Datla, R; *Inclusion of "Whisker Spray" Drag in Performance Prediction Method for High-Speed Planing Hulls*; Davidson Laboratory, Stevens Institute of Technology; Hoboken, NJ; Technical Report SIT-DL-06-9-2845; March 2006

Ikeda Yoshiho, T, Katayama; *Porpoising Oscillations of Very-High-Speed Marine Craft*; Mathematical, Physical & Engineering Sciences of the Royal Society, Series A, Vol. 358, No. 1771, pp.1905-1915, The Royal Institute of Naval Architects, UK. 2000

Ibrahim, R.A., Grace, I.M.; *Modeling of Ship Roll Dynamics and Its Coupling with Heave and Pitch*; Hindawi Publishing Corp. Mathematical Problems in Engineering Vol. 2010, Article ID 934714; 11 June 2009

Zubaly, R; *Applied Naval Architecture*; Cornell Maritime Press Inc., 1996

Dand, I; *The Effect of Water Depth on the Performance of High Speed Craft*; High Performance Yacht Design Conference, Auckland, 4-6 December 2002

ITTC Special Committee; *High Speed Marine Vehicle (HSMV);* ITTC- Recommended Procedures and Guidelines, Testing and Extrapolation Methods High Speed Marine Vehicles Resistance Test; 7.5-02-05-01 Revision 01. 2002

M.A. Ricciardo
matthew.ricciardo@gmail.com